Optica Applicata, Vol. LIII, No. 1, 2023
DOI: 10.37190/oa230111

Comparison of linear and circular polarization in foggy environments at UV-NIR wavelengths

XIANGWEI ZENG[1,*], YAHONG LI[2], XUEYE CHEN[1], HONGXIA ZHENG[1]

[1]College of Transportation, Ludong University, Yantai 264025, China

[2]Research Institute of Photonics, Dalian Polytechnic University, Dalian116034, China

[*]Corresponding author: zengxw163@163.com

This paper investigates the polarization persistence of linear polarization and circular polarization in foggy environments from ultraviolet (UV) to near-infrared (NIR). Using polarization tracking Monte Carlo simulation for varying particle size, wavelength, refractive index, and detection distance, it is shown that linear polarization and circular polarization exhibit different persistence performance. For wet haze of 0.6 μm mean diameter particles, right-handed circular polarization shows better persistence than parallel polarization at wavelengths of 0.36, 0.543 and 1.0 μm. But parallel polarization shows better persistence at wavelengths of 1.55, 2.1 and 2.4 μm. For wet haze of 1.0 μm mean diameter particles, right-handed circular polarization shows better persistence at wavelengths of 0.36, 0.543, 1.0 and 1.55 μm. But parallel polarization shows better persistence at wavelengths of 2.1 and 2.4 μm. For wet haze of 2.0 μm particles and radiation fog and advection fog, right-handed circular polarization shows better persistence at all simulated wavelengths. In short, right-handed circular polarization persists better than parallel polarization in most scenarios, however, with increasing wavelength and decreasing particle size, parallel polarization gradually persists better than right-handed circular polarization. Finally, anisotropy factor for various particle models is used to map the propagation law of right-handed circular polarization and parallel polarization.

Keywords: polarization, atmospheric scattering, forward scattering.

1. Introduction

Working in scattering environments, such as haze and fog, poses a serious challenge for most transport [1] and is important for many critical surveillance applications [2]. Scattering particles in haze and fog change the direction of radiation, reducing the radiation that reaches and returns from a target. This results in decreased signal from the target and ultimately a decrease in the ability to distinguish a target from the background. Polarized light's propagation has superior persistence in scattering environments. The use of polarized light has shown great performance for improving detection range and sensing in scattering environments [3–5].

Some of the first studies utilizing polarization to increase detection range in foggy environments date back to the 1960's. DEIRMENDJIAN numerically calculated linear polarization properties of water clouds (mean diameter = 5 μm) and hazes (mean diameter = 0.1 μm) models at limited specific wavelengths [6]. RYAN and CARSWELL performed experiments in laboratory-generated fog looking at linearly polarized light's persistence at a wavelength of 514 nm [7]. Measure results reveal that in dense fogs the linear polarization is strongly preserved in forward transmission. The research in this area has become a hot issue in the past ten years with decreasing cost of polarization detection. FADE *et al*. experimented in fog conditions of long-range polarimetric imaging a polarized 3000 K halogen incandescent source from a distance of 1.3 km [8]. They utilized only linear polarization for both illumination and polarimetric difference image, but were able to measure a maximum fourfold increase in contrast. VAN DER LAAN *et al*. simulated that circular polarization maintains its polarization state superiorly compared to linear polarization for radiation fog and advection fog in the visible and infrared spectrum [9]. They experimented in realistic fog environments at 532 and 1550 nm wavelengths and found out that circular polarization increased the contrast compared to linear polarization [10]. PEÑA-GUTIÉRREZ *et al*. experimented in 30 m fog chamber at visible bands and found out that circularly polarized light is demonstrated to be superior in forward transmission compared to the same phenomena with linearly polarized light [11].

While the potential impact to application is significant, the optical science and sensing community lacks data on broad wavelength to select linear polarization or circular polarization for increasing detection range and signal persistence. In this paper, we simulated the propagation of linear polarization and circular polarization in foggy environments at wavelengths of UV-NIR, especially focusing on polarized light's superior persistence in foggy environments.

2. Background

2.1. Retention rate of polarization state: RoPS

To describe the change in the polarization state of forward-scattered light, we defined a new parameter: RoPS (retention rate of polarization state) [12],

$$\mathrm{RoPS} = \frac{\pm P_{\eta\text{-forward}}}{P_{0\text{-forward}}} \tag{1}$$

where, $P_{0\text{-forward}}$ is the total intensity of the forward transmitted light; $P_{\eta\text{-forward}}$ is the intensity of the η type polarized light. η type polarized light has the same state of polarization as the initial light. ± represents the type of η type polarized light, which has a classification form similar to that of the Stokes parameters.

RoPS is Stokes–Mueller matrix transformation form, but it avoids the effect introduced by calculation of orthogonal component intensity difference. When evaluating

the polarization state characteristic of light waves during forward transmission, RoPS has higher calculation accuracy than Stokes parameters.

2.2. Polarization-tracking Monte Carlo

We used a meridian planes polarization-tracking Monte Carlo program to study forward transmission [13]. For these simulations, two polarization states were used, parallel polarized photons ($S = [1,1,0,0]^T$) and right circularly polarized photons ($S = [1,0,0,1]^T$). The polarization state of the photon is determined by decomposing the electric field into parallel and right-circular components with respect to the defined meridian plane. One million parallel or right-handed circular polarization photons were sent into a slab represented by one particular particle distribution for each environment. The photons were propagated at a given distance and then the aggregated polarization was calculated from the photons that arrived in a given area. After a scattering event, the photon direction is changed and a new meridian plane was found. The resulting scattered polarization state changes on the new meridian plane and the new parallel and right-circular electric field components. This process continues until the photon is scattered in or out the front or back face of the medium. Furthermore, the time of scattering is assumed to be ≤ 15 by considering the actual detector threshold. It is a maximum threshold for the maximum number of scatterings before a photon is killed in the model. The setting is a random setting and can be revised according to the detector threshold. Photons that exit the front face of the slab were considered as the transmitted photons. This process continued for all the photons that were launched. Then, the result was calculated by the formula (1).

3. Simulation environments

Three foggy environments were simulated: wet haze, radiation fog, and advection fog. For each environment, with different particle sizes, different wavelengths and identical relative humidity (90%) were set to simulate in variable distances.

Log-normal distribution can effectively describe the distribution of wet haze and fog [14]. In simulation, log-normal distribution was set as

$$f(d) = \frac{1}{\sqrt{2\pi}\,\sigma d} \exp\left[-\frac{(\ln d - \ln d_{\text{mean}})^2}{2\sigma^2}\right] \tag{2}$$

where d is the particle diameter, σ is the logarithmic standard deviation, and d_{mean} is the mean diameter. The logarithmic standard deviation was set as 0.1. The Table shows the mean diameter of foggy environments.

T a b l e. Three foggy environments and their granularity settings.

Type	Wet haze	Radiation fog	Advection fog
Mean diameter [μm]	0.6, 1, 2	5, 7.5, 10	15, 30, 45

In previous studies [12], we optimized certain spectral bands from ultraviolet to infrared. We selected wavelengths of 0.36, 0.543, 1.0, 1.55, 2.1 and 2.4 μm in simulation.

Furthermore, the transmission environment of right-handed circularly polarized photons and parallel polarized photons are same. However, the increase in particle size reduces the number of scattering, resulting in insignificant simulation results. To this end, the propagation distance was increased in advection fog. The maximum propagation distance was set at 100 m in wet haze and radiation fog, and 200 m in advection fog.

4. Results

Figure 1 shows results for wet haze of 0.6, 1 and 2 μm mean diameter droplets, respectively. For wet haze of 0.6 μm mean diameter particles, right-handed circular polarization shows better persistence than parallel polarization at wavelengths of 0.36, 0.543 and 1.0 μm. But parallel polarization shows better persistence at wavelengths of 1.55, 2.1 and 2.4 μm. For wet haze of 1.0 μm mean diameter particles, right-handed circular polarization shows better persistence at wavelengths of 0.36, 0.543, 1.0 and 1.55 μm. But parallel polarization shows better persistence at wavelengths of 2.1 and 2.4 μm. For wet haze of 2.0 μm particles, right-handed circular polarization shows better persistence at all simulated wavelengths.

Figure 2 shows results for radiation fog of 5, 7.5 and 10 μm mean diameter droplets, respectively. Right-handed circular polarization generally shows better persistence at all simulated wavelengths.

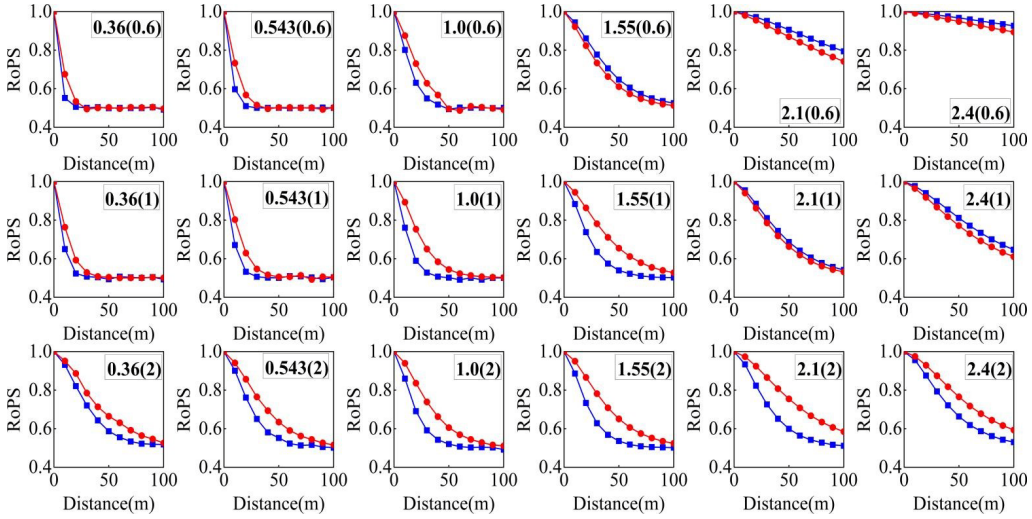

Fig. 1. RoPS of parallel and right-handed circular polarization in three simulated wet haze environments. RoPS values of parallel polarization are shown as blue lines. RoPS values of right-handed circular polarization are shown as red lines. Numbers in round brackets in each figure indicate the simulated wavelengths (particle diameter).

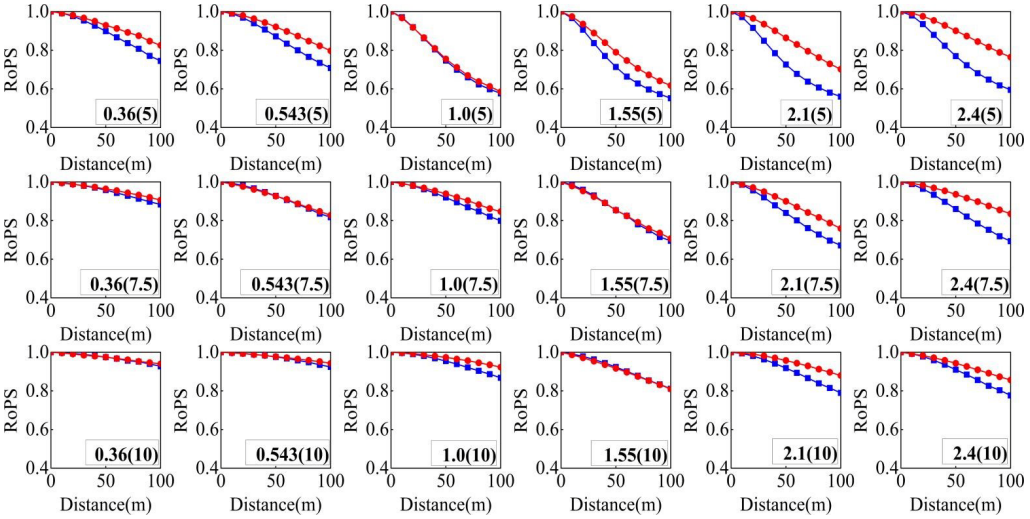

Fig. 2. RoPS of parallel and right-handed circular polarization in three simulated radiation fog environments. RoPS values of parallel polarization are shown as blue lines. RoPS values of right-handed circular polarization are shown as red lines. Numbers in round brackets in each figure indicate the simulated wavelengths (particle diameter).

Figure 3 shows results for advection fog of 15, 30 and 45 μm mean diameter droplets, respectively. Right-handed circular polarization generally shows better persistence in advection fog of 15 and 30 μm mean diameter droplets. But for the advective fog

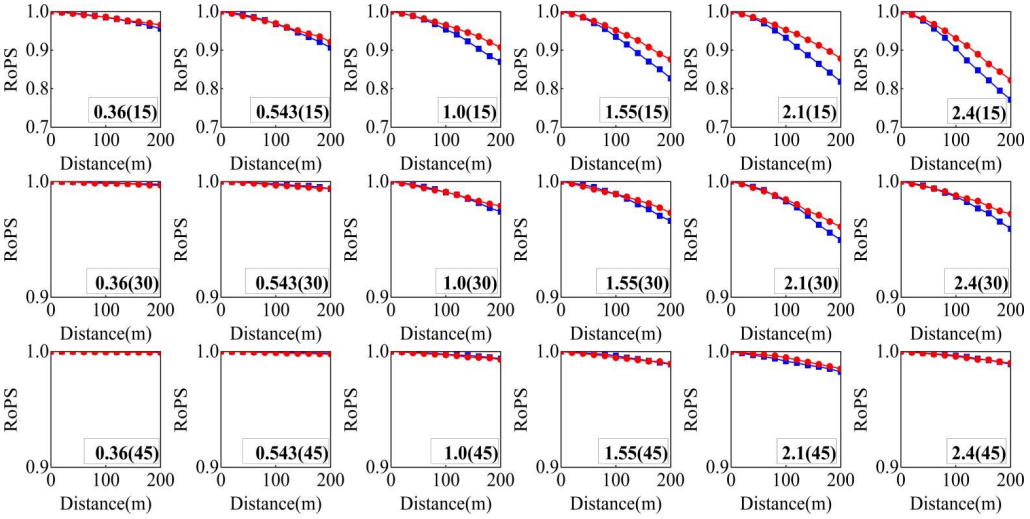

Fig. 3. RoPS of parallel and right-handed circular polarization in three simulated advection fog environments. RoPS values of parallel polarization are shown as blue lines. RoPS values of right-handed circular polarization are shown as red lines. Numbers in round brackets in each figure indicate the simulated wavelengths (particle diameter).

of 45 μm mean diameter droplets, right-handed circular polarization and parallel polarization have similar results. It is due to the simulated relative humidity which is consistent. Scattering events decrease with increasing particle size.

In short, right-handed circular polarization persists better than parallel polarization in most scenarios, however, with increasing wavelength and decreasing particle size, parallel polarization gradually persists better than right-handed circular polarization.

5. Discussion

The vector Fokker–Planck approximation shows that circular polarization memory has correlated with the anisotropy factor g [15]. Circular polarization retains its helicity and handedness when propagating in anisotropic random media. In comparison, the linear polarization state is randomized at a faster rate. This situation reverses as environmental anisotropy diminishes. Circular polarization easily flips handedness when the environment tends to be isotropic. In comparison, the linear polarization state is randomized at a slower rate.

We investigated the effects of anisotropy on circular polarization memory by studying a single particle. Figure 4 shows the relationship between anisotropy factor g and

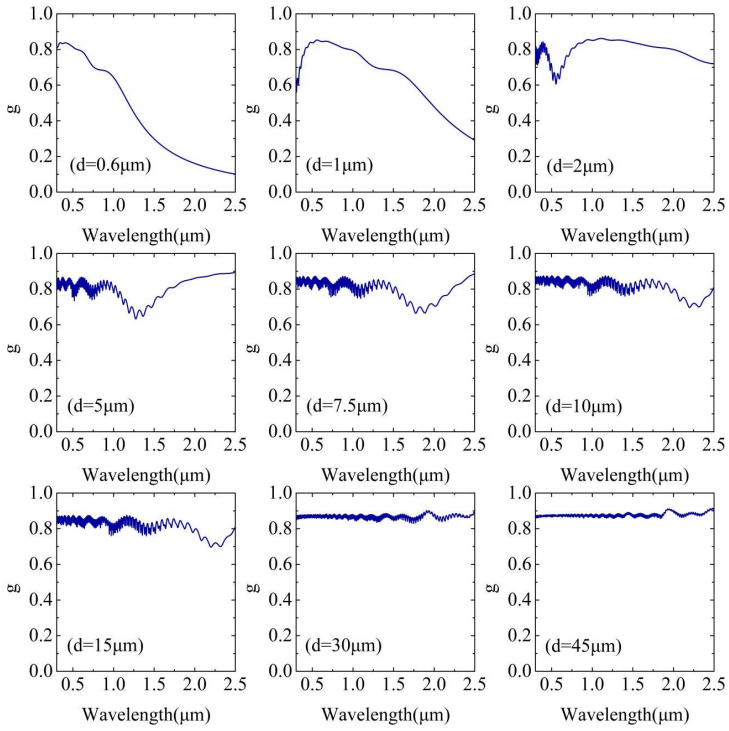

Fig. 4. The relationship between anisotropy factor g and wavelength in various particles (d is particle diameter).

wavelength in various particles. (1) For a particle of 0.6 μm diameter, the anisotropy factor basically shows a decreasing trend with increasing wavelength. The anisotropy factor is greater than 0.6 in the 0.3–1.0 μm band, but lower than 0.4 in the 1.25–2.5 μm band. (2) For a particle of 1.0 μm diameter, the anisotropy factor increases first and then decreases. The anisotropy factor is higher than 0.6 in the 0.3–1.5 μm band, but lower than 0.4 in the 2–2.5 μm band. (3) For a particle of 2.0 μm diameter and all the rest, the anisotropy factor remains stable in the range above 0.6.

Compared with the propagation law, parallel polarization persists better than right -handed circular polarization when the anisotropy factor is lower than 0.4, but right -handed circular polarization persists better than parallel polarization when the anisotropy factor is higher than 0.6. As expected, anisotropy factor for various particle models allows for basic mapping of the propagation law of right-handed circular polarization and parallel polarization. And as multiple scattering accumulates, it will be stable in the propagation law.

6. Conclusions

This work presents simulation quantifying persistence of linear polarization and circular polarization in various foggy environments at wavelengths of UV-NIR. Through polarization-tracking Monte Carlo simulation, we have shown that right-handed circular polarization persists better than parallel polarization in most scenarios, however, with increasing wavelength and decreasing particle size, parallel polarization gradually persists better than right-handed circular polarization. To verify the result, anisotropy factor of various particle models is used to map the propagation law of right-handed circular polarization and parallel polarization.

This work extends previously published works and offers new insight into potential realistic environments with broad wavelength ranges to polarization effect, *i.e*. of when linear polarization or circular polarization should be chosen to increase detection range.

Funding

This work was supported by Special Supporting Funds for National Natural Science Foundation of China (CN) (62105136), Special Supporting Funds for Leading Talents above Provincial Level in Yantai City (220-20230002), Ludong University introduced talents and started funding project (LD22065, LD23405).

Declaration of interests

The authors declare that they have no known competing financial interests or personal relationships that could have appeared to influence the work reported in this paper.

Data availability

Data underlying the results presented in this paper are not publicly available at this time but may be obtained from the authors upon reasonable request.

References

[1] JUDD K.M., THORNTON M.P., RICHARDS A.A., *Automotive sensing: Assessing the impact of fog on LWIR, MWIR, SWIR, visible, and lidar performance*, Proc. SPIE **11002**, Infrared Technology and Applications XLV, 2019: 110021F, DOI: 10.1117/12.2519423.

[2] TYO J.S., GOLDSTEIN D.L., CHENAULT D.B., SHAW J.A., *Review of passive imaging polarimetry for remote sensing applications*, Applied Optics **45**(22), 2006: 5453–5469, DOI: 10.1364/AO.45.005453.

[3] TUCHIN V.V., *Polarized light interaction with tissues*, Journal of Biomedical Optics **21**(7), 2016: 071114, DOI: 10.1117/1.JBO.21.7.071114.

[4] LERNER A., SHASHAR N., *Polarized Light and Polarization Vision in Animal Sciences*, Springer, Berlin, 2014.

[5] GUO Z., WANG X., LI D., WANG P., ZHANG N., HU T., ZHANG M., GAO J., *Advances on theory and application of polarization information propagation*, Infrared and Laser Engineering **49**(6), 2020: 20201013, DOI: 10.3788/IRLA20201013.

[6] DEIRMENDJIAN D., *Scattering and polarization properties of water clouds and hazes in the visible and infrared*, Applied Optics **3**(2), 1964: 187–196, DOI: 10.1364/AO.3.000187.

[7] RYAN J.S., CARSWELL A.I., *Laser beam broadening and depolarization in dense fogs*, Journal of the Optical Society of America **68**(7), 1978: 900–908, DOI: 10.1364/JOSA.68.000900.

[8] FADE J., PANIGRAHI S., CARRÉ A., FREIN L., HAMEL C., BRETENAKER F., RAMACHANDRAN H., ALOUINI M., *Long-range polarimetric imaging through fog*, Applied Optics **53**(18), 2014: 3854–3865, DOI: 10.1364/AO.53.003854.

[9] VAN DER LAAN J.D., SCRYMGEOUR D.A., KEMME S.A., DERENIAK E.L., *Detection range enhancement using circularly polarized light in scattering environments for infrared wavelengths*, Applied Optics **54**(9), 2015: 2266–2274, DOI: 10.1364/AO.54.002266.

[10] VAN DER LAAN J.D., SEGAL J.W., WESTLAKE K., REDMAN B.J., WRIGHT J.B., *Testing active polarimetric imagers in fog*, Sandia National Lab. (SNL-NM), Albuquerque, NM (United States), 2019.

[11] PEÑA-GUTIÉRREZ S., BALLESTA-GARCIA M., GARCÍA-GÓMEZ P., ROYO S., *Quantitative demonstration of the superiority of circularly polarized light in fog environments*, Optics Letters **47**(2), 2022: 242–245, DOI: 10.1364/OL.445339.

[12] ZENG X., CHEN X., LI Y., QIAO X., *Polarization enhancement of linearly polarized light through foggy environments at UV–NIR wavelengths*, Applied Optics **60**(26), 2021: 8103–8108, DOI: 10.1364/AO.431638.

[13] RAMELLA-ROMAN J.C., PRAHL S.A., JACQUES S.L., *Three Monte Carlo programs of polarized light transport into scattering media: part I*, Opt. Express. **13**(12), 2005: 4420–4438, DOI: 10.1364/OPEX.13.004420.

[14] JOHN W., *Size distribution characteristics of aerosols*, [In] *Aerosol Measurement: Principles, Techniques, and Applications, Third Edition*, P. Kulkarni, P.A. Baron, K. Willeke [Eds.], Wiley, 2011: 41–54, DOI: 10.1002/9781118001684.ch4.

[15] CLARK J.P., KIM A.D., *Forward-peaked scattering of polarized light*, Optics Letters **39**(22), 2014: 6422–6425, DOI: 10.1364/OL.39.006422.

Received June 1, 2022
in revised form July 9, 2022